Postharvest Biology and Technology 52 (2009) 1–8

Contents lists available at ScienceDirect

Postharvest Biology and Technology

journal homepage: www.elsevier.com/locate/postharvbio

Detecting chilling injury in Red Delicious apple using hyperspectral imaging and neural networks

Gamal ElMasry[a], Ning Wang[b,*], Clément Vigneault[b,c]

[a] Agricultural Engineering Department, Faculty of Agriculture, Suez Canal University, Ismailia, Egypt
[b] Department of Biosystems and Agricultural Engineering, Oklahoma State University, Stillwater, OK, USA
[c] Horticulture Research and Development Centre, Agriculture and Agri-Food Canada, 430 Gouin Boulevard, Saint-Jean-sur-Richelieu, Quebec, Canada

ARTICLE INFO

Article history:
Received 11 May 2008
Accepted 25 November 2008

Keywords:
Hyperspectral imaging
Artificial neural network (ANN)
Apple
Optimal wavelength
Firmness
Chilling injury

ABSTRACT

Hyperspectral imaging (400–1000 nm) and artificial neural network (ANN) techniques were investigated for the detection of chilling injury in Red Delicious apples. A hyperspectral imaging system was established to acquire and pre-process apple images, as well as to extract apple spectral properties. Feed-forward back-propagation ANN models were developed to select the optimal wavelength(s), classify the apples, and detect firmness changes due to chilling injury. The five optimal wavelengths selected by ANN were 717, 751, 875, 960 and 980 nm. The ANN models were trained, tested, and validated using different groups of fruit in order to evaluate the robustness of the models. With the spectral and spatial responses at the selected five optimal wavelengths, an average classification accuracy of 98.4% was achieved for distinguishing between normal and injured fruit. The correlation coefficients between measured and predicted firmness values were 0.93, 0.91 and 0.92 for the training, testing, and validation sets, respectively. These results show the potential of the proposed techniques for detecting chilling injury and predicting apple firmness.

1. Introduction

The world acreage of apple is 4,786,350 ha and the production is 63,875,324 tonnes (FAOSTAT, 2006). Generally, apple susceptibility to defects is affected by the nature of the variety, the growing conditions, the harvesting dates, postharvest treatment, and handling and storage conditions. External defects are usually easy to detect visually, especially when they present some contrast with normal tissues.

Chilling injury is among the most common disorders recognized by industry during the past few years. It is physiological damage to fruit cell membranes that may occur at any time due to harmful environmental conditions during the growing season, transportation, distribution, or storage, at the retail store, or even in a home refrigerator. Membrane damage is often followed by a cascade of secondary effects, such as ethylene production, an increase in respiration, a decrease in photosynthesis, and an alteration of cellular structure causing the fruits to be more susceptible to diseases. This injury first appears as a very slight browning discoloration of the flesh, sometimes accompanied by core browning. The discoloration is often ignored by untrained inspectors. As a result, the affected fruit can be misclassified as normal. However, chilling injury disorder of apples can progress quickly to make the fruit unmarketable (Watkins and Jackie Nock, 2004). Early detection and diagnosis of chilling injury is rather difficult, as the injured produce often looks sound as long as it remains in low temperatures. Symptoms become evident when the produce is placed in warmer temperatures. They may appear almost immediately, or take several days to develop (Skog, 1998). Damage in fruit cell membranes due to chilling injury affect normal firmness and lead the fruit to gain spongy texture. As a consequence, firmness change could be used as an indication of possible chilling injury. Increased demands for objectivity, consistency, and efficiency in defect detection techniques have necessitated the introduction of computer-based techniques that can substitute human inspection. The techniques should be rapid, precise, reliable and non-destructive. Hyperspectral imaging integrates spectroscopy and digital imaging techniques to provide spectral and spatial information simultaneously for the surface of interest on a target object. A hyperspectral image consists of a series of sub-images, each one representing the intensity distribution at a certain spectral band. When a fruit is exposed to light, about 4% of the incident light is reflected at the outer surface, causing specular reflectance, and the remaining incident energy is transmitted through the surface into the cellular structure of the produce where it is scattered by the small interfaces within the tissue or absorbed by cellular constituents (Birth, 1976). The reflected and re-emitted radiation can be measured and recorded as an absorption/reflectance spectrum (Bochereau et al., 1992). This spectrum is related to the chemical composition of the fruit, and

* Corresponding author. Tel.: +1 405 744 2877; fax: +1 405 744 6059.
E-mail address: ning.wang@okstate.edu (N. Wang).

0925-5214/$ – see front matter © 2008 Elsevier B.V. All rights reserved.
doi:10.1016/j.postharvbio.2008.11.008

spectra collected from fruit at different quality levels can therefore be quite different. Hyperspectral imaging is advantageous relative to spectroscopic techniques, which acquire the spectral data from a single point or from an integration of a small region on the tested fruit. Hyperspectral imaging acquires spatially distributed spectral responses at pixel levels, which allows flexible selection of regions of interest on a target object, e.g. variable sizes and locations. By incorporating adaptive algorithms, defect detection performance by hyperspectral imaging can be greatly improved. Hyperspectral imaging has been implemented in several applications, such as the inspection of poultry carcasses (Chao et al., 2001; Park et al., 2004), defect detection in apple (Mehl et al., 2004), chilling injury detection in cucumber (Liu et al., 2006), quality determination in fruits and vegetables (Kim et al., 2002; Polder et al., 2002; Cheng et al., 2004), estimation of physical and chemical properties in strawberry (Nagata et al., 2005), and firmness and soluble solids prediction in apple (Lu, 2004).

Artificial neural networks (ANN) have proven to be very effective in identification and classification of agricultural produce (Bochereau et al., 1992; Jayas et al., 2000), where non-coherence or non-linearity often exists. Kavdır and Guyer (2002, 2004) developed a back-propagation neural network (BPNN) with the textural features extracted from spatial distribution of color/gray levels to detect defects (leaf roller, bitter pit, russet, puncture and bruises) in Empire and Golden Delicious apples. Barreiro et al. (1997) tested different neural network approaches for bruise prediction in apple, pear and peach. Park and Chen (1996) integrated a feed-forward back-propagation ANN and a spectral imaging technique to separate wholesome chicken carcasses from unwholesome ones. The classification accuracies were 100% for calibration and 93.3% for validation. Hahn et al. (2004) analyzed visible and near-infrared spectra with a neural network for the detection of fungal rots in tomato. They reported that 96% of the infected tomato fruit were properly detected. Kim et al. (2000) compared the performance of a linear pattern recognition technique (i.e. linear discrimination analysis) with that of non-linear techniques based on multilayer perceptrons with variations on back-propagation learning to classify kiwi fruit grown under different conditions. It was concluded that ANNs appeared to be well suited to the classification of fruit grown or stored under different conditions.

The main objective of this study was to establish sufficiently robust models for the detection of chilling injury in Red Delicious apple using the tools of hyperspectral imaging and artificial neural networks. The specific objectives were: (a) to categorize spectral signatures for normal and chilling-injured Red Delicious apples; (b) to establish an ANN model for the selection of the optimal wavelength(s) for segregating normal apples versus injured apples; (c) to develop ANNs for monitoring firmness changes in Red Delicious apples based on spectral images at the selected optimal wavelength(s); and (d) to develop ANNs for fruit classification according to firmness levels.

2. Materials and methods

2.1. Apple samples

Red Delicious apples were purchased from local retail stores. A total of 64 apples free from any abnormal features such as defects, bruises, diseases and contamination were selected. Chilling injury was stimulated in 32 apples by keeping them in a cold storage at −1 °C for 24 h. The injured apples were removed from the cold storage and kept at room temperature (20 ± 1 °C) for another 24 h to allow injury development. The other 32 apples were stored at room temperature (20 ± 1 °C) and used as control (normal) samples. The chilling injury developed from this method resulted in injuries in various locations in the checked area along the equatorial zone and also beside the stem and calyx regions of the apple. The external surface of the injured apples looked visually normal in terms of color and texture. All 64 apples (normal and injured) were used for training and testing an ANN for the selection of the optimal wavelength(s). To increase the robustness of the developed ANN models, another 20 Red Delicious apples were purchased in order to validate the ANN models and algorithms that were developed. Among the 20 apples, chilling injuries were stimulated on 10 apples using the previously described procedures. The other 10 apples were kept at room temperature and used as normal apples.

2.2. Hyperspectral imaging system

Hyperspectral images of the apples (normal and injured) were acquired using a lab-scale hyperspectral imaging system (Fig. 1) that consisted of a charge-coupled device (CCD) camera (PCO-1600, PCO Imaging, Germany) connected to a spectrograph (ImSpector V10E, Optikon Co., Canada) coupled with a standard C-mount zoom lens. The optics of this imaging system allowed studying fruit properties associated with the spectral range of 400–1000 nm. The camera faced downward at a distance of 400 mm from the target. The sample was illuminated through a cubic tent made of white nylon fabric to provide uniform lighting conditions. The light source consisted of two 50 W halogen lamps mounted at a 45° angle from horizontal, fixed at 500 mm above the sample and spaced 900 mm apart on two opposite sides of the sample. The sample was put in a position that corresponded with the center of the field of view of the camera (300 mm × 300 mm), with calyx–stem end perpendicular to the camera lens to avoid any discrepancy between the normal surface and stem or calyxes. The camera-spectrograph assembly was provided with a stepper motor to move this unit through the camera's field of view to scan the apple line-by-line.

The spectral images were collected in a dark room where only the halogen light source was used. The exposure time was adjusted to 200 ms throughout the test. Each collected spectral image was stored as a three-dimensional image (x, y, λ). The spatial components (x, y) included 400 × 400 pixels, and the spectral component (λ) included 826 bands within 400–1000 nm range. The hyperspectral imaging system was controlled by a laptop Pentium M computer (processor speed: 2.0 GHz; RAM: 2.0 GB) preloaded and configured with the Hypervisual Image Analyzer® software program (ProVision Technologies, Stennis Space Center, MO, USA). All spectral images acquired were processed and analyzed using the

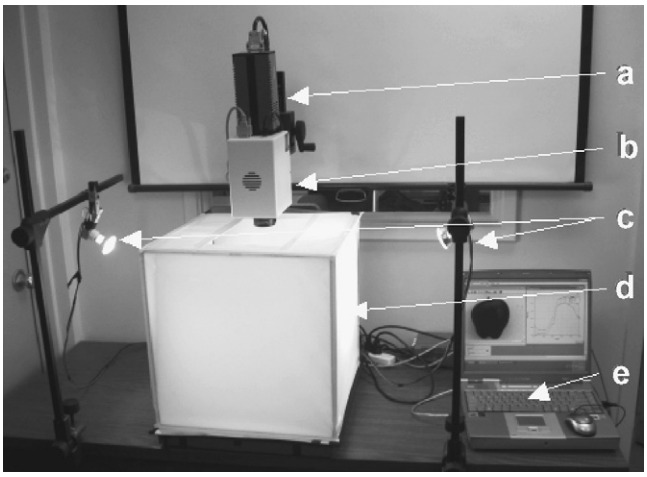

Fig. 1. The hyperspectral imaging system: (a) a CCD camera; (b) a spectrograph with a standard C-mount zoom lens; (c) an illumination unit; (d) a light tent; and (e) a PC supported with the image acquisition software.

Environment for Visualizing Images software program (ENVI 4.2, Research Systems Inc., Boulder, CO, USA).

The hyperspectral images were calibrated with a white and a dark references. The dark reference was used to remove the dark current effect of the CCD detectors, which are thermally sensitive. The calibrated image (R) was then defined using the following equation (Mehl et al., 2002; Xing and De Baerdemaeker, 2005):

$$R = \frac{R_o - D}{W - D} \times 100 \quad (1)$$

where R_o is the acquired hyperspectral image, D is the dark image (with 0% reflectance) collected by turning off the light source by means of completely closing the lens of the camera, and W is the white reference image taken from a standard white reference board (Teflon white board with 99% reflectance). The calibrated images were used to extract information about the spectral properties of normal and injured apples with a view to optimizing the identification of chilling injury, the selection of effective wavelengths, the prediction of firmness, and classification.

2.3. Hyperspectral image acquisition

By using this hyperspectral imaging system, two hyperspectral images were acquired for each fruit in the training, testing and validation sets: one image was acquired for the intact apple and the other image, named "flesh image", was recorded when the peel was completely removed from the fruit with a sharp knife. The flesh images were used to compare the characteristics and spectral signatures with the intact apples under normal and injured conditions.

2.4. Extraction of apple spectral properties

The first step in detecting chilling injury was to extract the spectral signatures representing chilling-injured apples and those representing normal apples. The detailed steps in extracting the spectral signature are illustrated in Fig. 2. Since one spectral image consisted of 826 sub-images of different intensities, the sub-image which presented the apple more contrasted compared with background were picked up to isolate the apple using global thresholding. Therefore, the sub-image at 550 nm, which represented the best contrast between the apple and background, was selected from the spectral space (826 sub-images) and segmented to act as a mask for excluding the background pixels. The white pixels in the mask were used as an area of interest (AOI) to extract the spectral data from the calibrated hyperspectral image. The mean reflectance spectrum from the AOI of each hyperspectral image was calculated by averaging the spectral value of all pixels in the AOI. In total, 64 average spectra (400–1000 nm) representing the 64 tested apples were calculated and stored for selection of the wavelength and development of the ANN model. The same procedure was also used to obtain the spectral signature of the apple flesh by extracting spectral feature from flesh images.

2.5. Fruit color measurement

To demonstrate the visual changes that occurred during chilling injury development, fruit color was measured for both the external peel and the internal flesh. The color image was constructed for each apple by combining the red (650 nm), green (500 nm) and blue (450 nm) band images from the calibrated hyperspectral data space to form an RGB (red–green–blue) image. All RGB images were transformed into the L*a*b* color space, where L* stood for color lightness (0 indicates black and 100 indicates white), a* defined the position between green and red (0 indicates green and 255 indicates red), and b* indicated the position between blue and yellow (0 indicates blue and 255 indicates yellow). The RGB values were transformed into a* and b* color components in order to produce a better identification of color changes according to Vízhányó and Felföldi (2000). The color conversion process was conducted by means of a program written using MATLAB 7 (Release 14, The MathWorks Inc., MA, USA).

2.6. Firmness measurement

After spectral image acquisition, the firmness of each apple was measured with an Instron Universal Testing Machine (Model 4502, Series IX Automated Materials Testing System, Instron Corporation, MA, USA) using an 11-mm diameter plunger according to the standard method (ASAE, 1994). The plunger was pressed into the apple flesh to a depth of 9 mm at a speed of 0.83 mm s^{-1}. The maximum force extracted from the force-deformation curve was used to indicate the apple firmness. The firmness test was conducted at two opposite positions on the equator of the apple surface and subsequently averaged. The average maximum force was used as the firmness index of the apple.

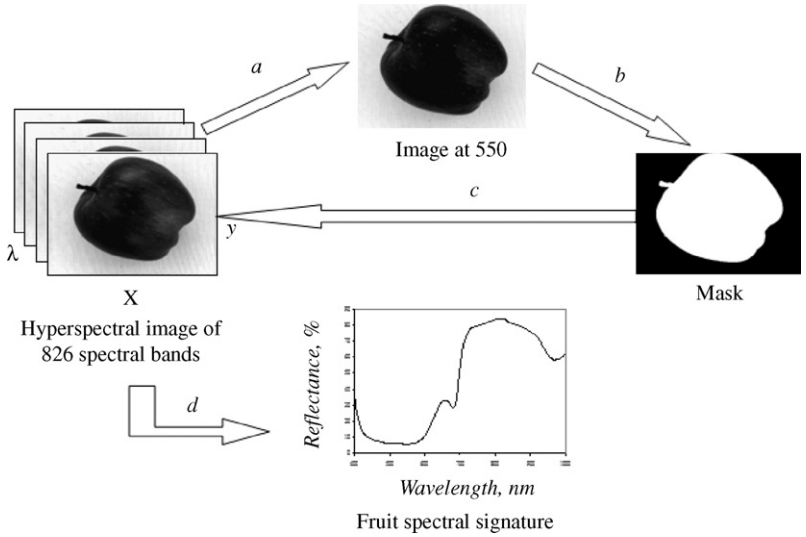

Fig. 2. Extraction of the fruit spectral signature: (a) selecting 550 nm image, (b) binarization (defining the AOI); (c) applying the mask; and (d) calculating the fruit spectral signature using only those at the white pixels in the mask.

2.7. Data volume reduction and optimal wavelength selection

The major disadvantage of the hyperspectral imaging technique is that handling the huge amount of data extracted from hyperspectral images requires extra time and resources. It is imperative that efficient manipulation procedures be used to reduce data dimensionality to its lowest level without losing functionality. In this study, instead of using the entire image volume ($400 \times 400 \times 826$), a reduced data cube with dimensions of $400 \times 400 \times n$, where n was the number of selected optimal wavelengths, was formed. The success of a classification algorithm based on the reduced data cube depended on the quality of the selection of the optimal wavelengths at which the spectral signatures could best describe each class. Although several wavelength selection techniques have been derived by researchers (e.g. Hruschka, 2001; Kim et al., 2002; Liu et al., 2003; Keskin et al., 2004; Mehl et al., 2004; Chong and Jun, 2005), the choice of a particular method depends on the nature of the problem, the size of the data set, ease of implementation and economic feasibility. In this study, an ANN was used for data volume reduction and wavelength selection on the basis of the fact that the network can change and adjust its knowledge by adjusting its weights according to the presented samples of data.

2.8. ANN Model 1 for selection of wavelength(s)

A multilayer BPNN, ANN Model 1, was developed to differentiate injured apples from normal ones (Fig. 3). Back-propagation was a canonical feed-forward network in which an error signal was fed back through the network, altering weights. BPNN was therefore a numerically intensive technique. Weights among the simple processing units of nodes were adjusted by iterating input patterns throughout the network until the error between the network output and the targeted output was minimized (Glorfeld, 1996). ANN Model 1 consisted of three layers: an input layer, an output layer and a hidden layer. The input layer had 826 nodes representing the spectral responses of an apple at each of the 826 wavelengths. Due to the large volume of data, only one hidden layer with five nodes was used. The number of nodes on the output layer was determined predominantly by the number of classes under investigation. Thus, two nodes were used: normal apples (coded as 1) and injured apples (coded as 0). A sigmoid function was used as a transfer function between the input and hidden layers, and a linear transfer function was used between the hidden and output layers. The network was trained for at least 20,000 epochs or until the error measurement approached 0.01%.

Among the 64 tested apples, 42 apples (both normal and injured) were randomly chosen as a training set to train the ANN model.

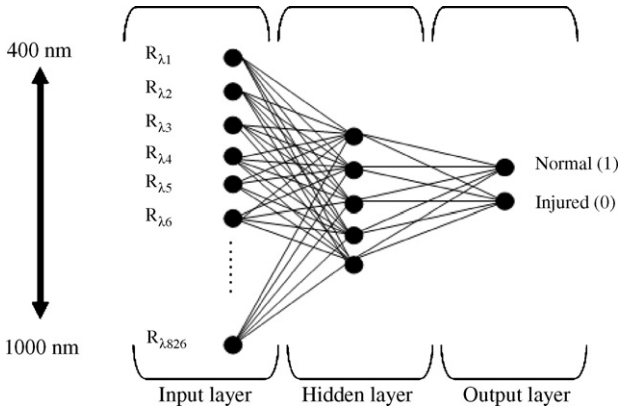

Fig. 3. Layout of ANN Model 1 for data dimensionality reduction and optimal wavelength selection.

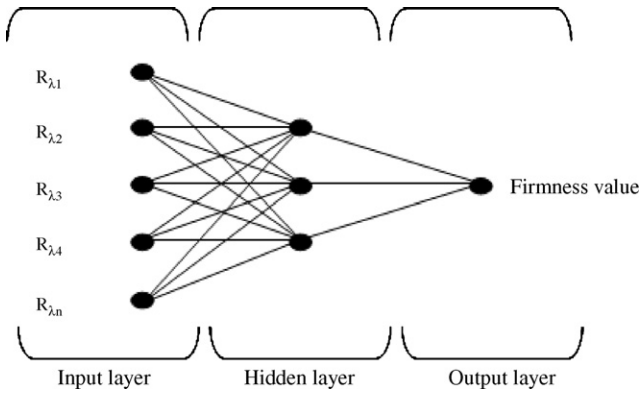

Fig. 4. A schematic depiction of a multilayer neural network for firmness prediction using the reflectance features at the optimal wavelengths as inputs.

The other 22 apples (both normal and injured) were used to test the model. This procedure was run three times on the same 64 apples; each time, 42 different apples were randomly selected for training, and the rest were used for testing. The outcomes of the three replications were averaged to calculate the importance of each variable.

The importance of each variable (wavelength) for the ANN model was evaluated using an index calculated by the following equation (Glorfeld, 1996):

$$M = \frac{\sum_{j=1}^{n_H} \left[\left(|I|_{p_j} / \sum_{k=1}^{n_p} |I|_{p_{j,k}} \right) |O|j \right]}{\sum_{i=1}^{n_p} \left(\sum_{j=1}^{n_H} \left[\left(|I|_{p_{i,j}} / \sum_{k=1}^{n_p} |I|_{p_{i,j,k}} \right) |O|j \right] \right)} \quad (2)$$

where M is the importance measure for the input variable, n_p is the number of input variables (826), n_H is the number of hidden layer nodes (five nodes), $|I|_{p_j}$ is the absolute value of the hidden layer weight corresponding to the pth input variable and the jth hidden layer, and $|O|_j$ is the absolute value of the output layer weight corresponding to the jth hidden layer.

Each input variable had five weights corresponding to the five nodes in the hidden layer of the ANN. The index M value was calculated for each input node and then normalized in the 0–1 range. The higher the M value, the more important the node (variable/wavelength) was for the classification of injured and normal apples.

2.9. ANN Model 2 for firmness prediction

Based on the number of wavelengths selected by ANN Model 1, the second feed-forward BPNN, ANN Model 2 was established to predict the firmness of the apples. The input layer consisted of the reflectance features at the selected optimal wavelengths (Fig. 4). The hidden layer contained three nodes. The output layer contained only one node to represent the apple firmness value. Sigmoid and linear functions were used as transfer functions, and over-fitting was avoided by using a Bayesian regularization training algorithm. The model was trained using 42 randomly selected apples and tested with the remaining 22 apples. The maximum number of iterations in training was set to 5000.

2.10. ANN Model 3 for classification of apples

ANN Model 3 was a revised version of ANN Model 2. The spectral responses at the five optimal wavelengths were used as input nodes. The output layer was modified to have two nodes: normal and injured classes. The network was trained using 42 randomly selected apples and tested with the remaining 22

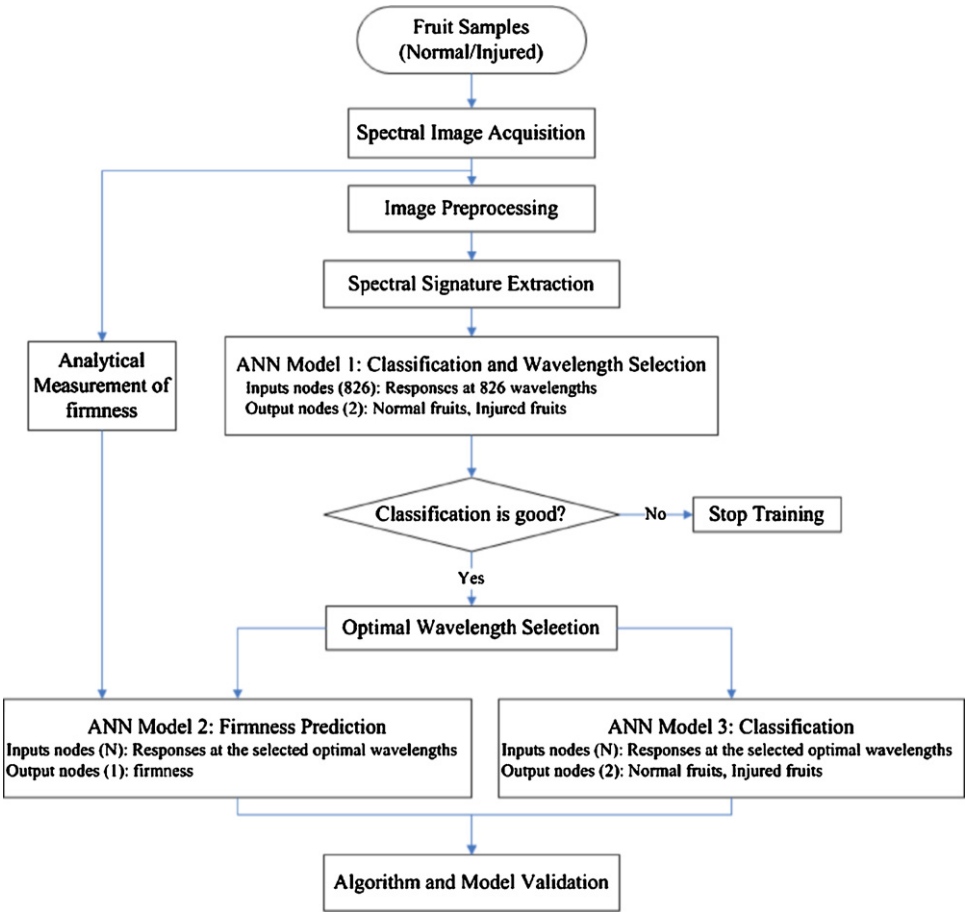

Fig. 5. Flowchart of the key steps involved in chilling injury detection algorithm.

apples, with each group containing both normal and injured apples. The maximum number of iterations in training was set to 5000.

The detailed procedures for detecting chilling injury and firmness changes in apples are illustrated in Fig. 5.

2.11. Test for robustness of the ANN models

The capability of the three ANN models for optimal wavelength selection, firmness prediction and classification was validated with a group of 20 apples purchased at a later stage in the experiment and called the validation set. Chilling injury was stimulated in 10 apples using the same method described previously. The same procedures were used for hyperspectral image acquisition, image pre-processing and firmness measurement. Model robustness was evaluated by comparing the correlation coefficients between the predicted and the actual firmness and among the classification accuracies obtained from the training, testing and validation sets.

2.12. Statistical analysis

The experimental results of color measurements and model evaluation were analyzed statistically using statistical toolbox of MATLAB 7 (Release 14, The MathWorks Inc., MA, USA). The calculations were performed at the significance level of $\alpha \leq 0.05$.

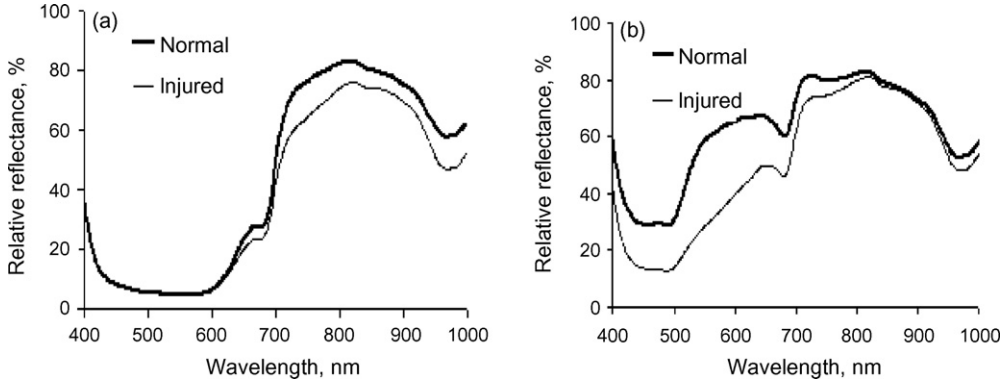

Fig. 6. Spectral characteristics of normal and injured apples for (a) the external surface and (b) the internal flesh.

3. Results and discussion

3.1. Spectral characteristics

Fig. 6a shows the average spectral signature of both normal and injured apples obtained from the apple surfaces. There were no significant differences between the normal and the injured apples in the visible range (400–700 nm), indicating that it was impossible to detect injured apples using machine vision systems that utilize gray-scale or color cameras. However, the distinction between normal and injured apples was obvious in the near-infrared region (700–1000 nm) due to chemical changes that occurred during chilling injury development. The internal spectral responses of the apple flesh that were obtained after removal of the peel are also illustrated (Fig. 6b). The difference between the flesh responses of both classes was clear, especially in the visible range, due to the browning effect of chilling injury development.

3.2. Color differences

The color differences between normal and injured apples for the external surface as well as for the internal flesh are shown in Table 1. The external surface (apple peel) exhibited the same appearance for both normal and injured apples, because there were no significant differences between the two classes for all color parameters (R, G, B, L*, a*, and b*). The results presented in Table 1 were in agreement with the spectral signatures of the apples in the visible range shown in Fig. 6a. However, there was a significant difference between the flesh of the normal apples and the flesh of the injured apples in all color parameters. If parameter a* is considered to be an indicator of browning (0 indicates green while 255 indicates red), the effect of chilling injury in terms of flesh browning can be evaluated. The a* value of normal flesh was 148.13 ± 2.98, which significantly differed from that of the injured flesh (159.76 ± 5.19). The higher a* value of injured apples indicated browning of the flesh compared with the flesh of the normal apples. Based on the spectral and color characteristics of normal and injured apples, it could be inferred that distinguishing injured apples from sound ones by means of visual methods is rather difficult.

3.3. Optimal wavelength selection

ANN Model 1 used the spectral responses on the entire spectral range (400–1000 nm) with 826 wavelengths and demonstrated excellent performance for detecting chilling injury effect, with 100% classification success for both the training and the testing samples. Fig. 7 presents the results obtained, along with the highest *M* values. The wavelengths corresponding to the highest *M* values, 717, 751, 875, 960 and 980 nm, were chosen as the optimal wavelengths. "Optimal" wavelength(s) was used to denote to wavelength(s) that was/were sensitive to any physicochemical changes that occurred in the apples during chilling injury. Firmness was indirectly related to various attributes in the apples. Hence, differences between normal and injured apples in terms of their firmness were investigated. The same wavelengths used for discriminating apple classes could also be suitable for firmness changes due to chilling injury.

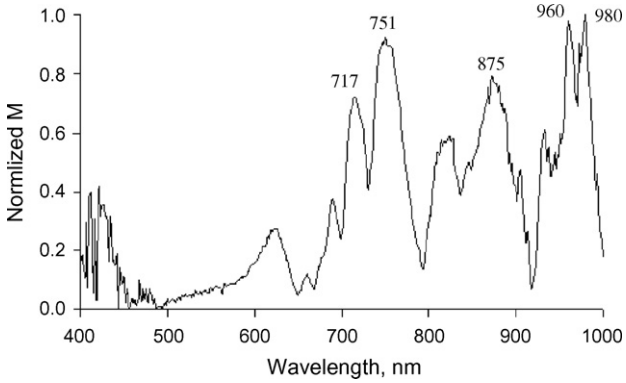

Fig. 7. The importance measure (*M*) values used to select the optimal wavelengths.

Table 2
Confusion matrix for fruit classification using ANN Model 3.

From/to	Normal	Injured	Total	% Correct
Normal	32	0	32	100
Injured	1	31	32	96.9
Total	33	31	64	98.4

3.4. Firmness prediction

Fig. 8a shows the performance of ANN Model 2 for firmness prediction of the training (42 apples) and the testing (22 apples) sets. The correlation coefficient between measured and predicted firmness values was 0.93 and 0.91 for the training and testing sets, respectively. The root mean square error (RMSE) was 8.26 and 9.40 N for the training and testing sets, respectively. Because of the high correlation coefficient of ANN Model 2 for firmness prediction, this model could be applied to the detection of firmness change due to chilling injury effect. Table 2 shows the confusion matrix for the classification of the 64 apples (training + testing) into normal and injured classes. A high classification accuracy of 98.4% was obtained with ANN Model 3.

3.5. Model robustness

Fig. 8b shows apple firmness predicted by ANN Model 2 for the validation set. The correlation coefficient between the actual and predicted firmness for the validation set was 0.92 with an RMSE value of 10.09 N. For classification, ANN Model 3 achieved 100%

Table 1
Means and standard deviations (S.D.) of color characteristics of normal and chilling-injured fruits for surface and flesh.

	External surface		Internal flesh	
	Normal Mean ± S.D.	Injured Mean ± S.D.	Normal Mean ± S.D.	Injured Mean ± S.D.
r[a]	0.626 ± 0.045a	0.616 ± 0.037a	0.814 ± 0.021a	0.735 ± 0.050b
g	0.187 ± 0.024a	0.198 ± 0.019a	0.557 ± 0.023a	0.395 ± 0.065b
b	0.187 ± 0.022a	0.186 ± 0.020a	0.218 ± 0.026a	0.118 ± 0.035b
L*	51.740 ± 8.57a	52.460 ± 8.09a	164.88 ± 4.50a	132.75 ± 14.61b
a*	156.86 ± 6.61a	155.93 ± ±5.54a	148.13 ± 2.98a	159.76 ± 5.19b
b*	144.64 ± 4.82a	144.77 ± 4.40a	182.21 ± 1.43a	180.13 ± 3.12b

Values with the same letters within the same row and characteristic are not significantly different, $\alpha = 0.05$.

[a] $r = \frac{R}{R+G+B}$; $g = \frac{G}{R+G+B}$; $b = \frac{B}{R+G+B}$.

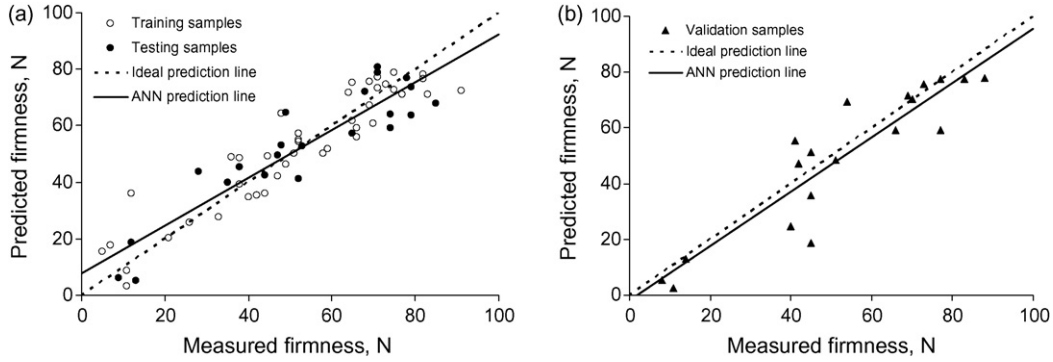

Fig. 8. Apple firmness prediction by neural network for (a) the training and testing sets and (b) the validation set.

success for categorization of the validation set into the two classes (normal and injured). Both results are therefore in agreement with the training and testing sets, indicating the robustness of the models for classification and firmness prediction of normal and injured Red Delicious apples.

3.6. Potential for production line implementation

The research conducted with the lab-scale hyperspectral imaging system provided the optimal wavelengths to be used in an industrial-scale multispectral imaging system for identifying chilling injured apples. The outcomes from this research show that based on the spectral responses at the selected optimal wavelengths and using the firmness and color changes as key parameters, chilling injured apples can be identified. To fine tune the selection of optimal wavelengths and the developed ANN models, more tests will be conducted with apple samples from different origins, at different ages, and with different level of chilling injuries. This will further improve the repeatability and reproductively of the developed ANN models.

During the experiments of current study, all apple samples were intentionally placed in the light tent with a controlled orientation with the calyx–stem perpendicular to the camera lens to avoid any discrepancy between the normal surface and stem or calyxes. In production line applications, a testing station with the multispectral system could be established at a selected location. A uniform lighting system and a specially designed sample holder could also be designed to eliminate edge and shadow effects and have some control on apple orientation. Such arrangements have proven effective in several industrial-scale image-based apple sorting systems.

4. Conclusions

A hyperspectral imaging system with a spectral range of 400–1000 nm was used for the detection of chilling injury in Red Delicious apples. There was no significant difference between normal and injured apples in terms of color parameters (R, G, B, L*, a*, and b*). Five optimal wavelengths (717, 751, 875, 960 and 980 nm) were selected by an artificial neural network model (Model 1) based on the maximum weight assigned to the input nodes. With the selected optimal wavelengths instead of the whole spectral range (826 wavelengths), the correlation coefficients between the actual and predicted firmness obtained using ANN Model 2 were 0.93, 0.91 and 0.92 for the training, testing and validation sets, respectively. ANN Model 3 achieved an accuracy of 98.4% and 100% in distinguishing normal from injured apples for the training + testing set and the validation set, respectively.

In summary, the experimental results demonstrated that a spectral imaging system associated with ANN can successfully distinguish between chilling-injured apples and normal apples, as well as detect firmness changes. In essence, it is rather unpractical to establish a hyperspectral system with very narrow spectral resolution (~0.73 nm) in on-line applications. Instead, multispectral imaging (using only the selected optimal wavelengths) could solve the problem of speed requirements. Considering the importance of the data volume reduction obtained, spectral imaging systems using the selected wavelengths open a new avenue for application in commercial implementations to detect various quality disorders in produce.

References

ASAE, 1994. Compression test of food materials of convex shape. In: ASAE Standards. ASAE, St. Joseph, MI, USA, ASAE S368.2, pp. 472–475.

Barreiro, P., Steinmetz, V., Ruiz-Altisent, M., 1997. Neural bruise prediction models for fruit handling and machinery evaluation. Computers and Electronics in Agriculture 8 (1), 91–103.

Birth, G.S., 1976. How light interacts with foods. In: Gafney, J.J. (Ed.), Quality Detection in Foods. ASAE, St. Joseph, MI, USA.

Bochereau, L., Bourgine, P., Palagos, B., 1992. A method for prediction by combining data analysis and neural networks: application to prediction of apple quality using near infra-red spectra. Journal of Agricultural Engineering Research 51 (2), 207–216.

Chao, K., Chen, Y.R., Hruschka, W.R., Park, B., 2001. Chicken heart disease characterization by multi-spectral imaging. Transactions of the ASAE 17 (1), 99–106.

Cheng, X., Chen, Y.R., Tao, Y., Wang, C.Y., Kim, M.S., Lefcourt, A.M., 2004. A novel integrated PCA and FLD method on hyperspectral image feature extraction for cucumber chilling damage inspection. Transactions of the ASAE 47 (4), 1313–1320.

Chong, L.G., Jun, C.H., 2005. Performance of some variable selection methods when multicollinearity is present. Chemometrics and Intelligent Laboratory Systems 78 (1), 103–112.

FAOSTAT, 2006. Food and agriculture organization of the United Nations for a world without hunger. http://faostat.fao.org/site/567/DesktopDefault.aspx?PageID=567#ancor. Web site visited on November 24, 2008.

Glorfeld, L.W., 1996. A methodology for simplification and interpretation of backpropagation-based neural network models. Expert Systems with Applications 10 (1), 37–54.

Hahn, F., Lopez, I., Hernandez, G., 2004. Spectral detection and neural network discrimination of *Rhizopus stolonifer* spores on red tomatoes. Biosystems Engineering 89 (1), 93–99.

Hruschka, W.R., 2001. Data analysis: wavelength selection methods. In: Norris, W.P. (Ed.), Near-Infrared Technology in the Agricultural and Food Industries. American Association of Cereal Chemists.

Jayas, D.S., Paliwal, J., Visen, N.S., 2000. Multi-layer neural networks for image analysis of agricultural products. Journal of Agricultural Engineering Research 77 (2), 119–128.

Kavdır, İ., Guyer, D.E., 2002. Apple sorting using artificial neural networks and spectral imaging. Transaction of the ASAE 45 (6), 1995–2005.

Kavdır, İ., Guyer, D.E., 2004. Comparison of artificial neural networks and statistical classifiers in apple sorting using textural features. Biosystems Engineering 89 (3), 331–344.

Keskin, M., Dodd, R.B., Han, Y.J., Khalilian, A., 2004. Assessing nitrogen content of golf course turfgrass clippings using spectral reflectance. Applied Engineering in Agriculture 20 (6), 851–860.

Kim, J., Mowat, A., Poole, P., Kasabov, N., 2000. Linear and non-linear pattern recognition models for classification of fruit from visible–near infrared spectra. Chemometrics and Intelligent Laboratory Systems 51, 201–216.

Kim, M.S., Lefcourt, A.M., Chao, K., Chen, Y.R., Kim, I., Chan, D.E., 2002. Multispectral detection of fecal contamination on apples based on hyperspectral imagery: Part I. Application of visible and near–infrared reflectance imaging. Transactions of the ASAE. 45 (6), 2027–2037.

Liu, Y., Windham, W.R., Lawrence, K.C., Park, B., 2003. Simple algorithms for the classification of visible/near-infrared and hyperspectral imaging spectra of chicken skins, feces, and fecal contaminated skins. Applied Spectroscopy 57 (12), 1609–1612.

Liu, Y., Chen, Y.R., Wang, C.Y., Chan, D.E., Kim, M.S., 2006. Development of hyperspectral imaging technique for the detection of chilling injury in cucumbers; spectral and image analysis. Applied Engineering in Agriculture 22 (1), 101–111.

Lu, R., 2004. Multispectral imaging for predicting firmness and soluble solids content of apple fruit. Postharvest Biology and Technology 31 (1), 147–157.

Mehl, P.M., Chao, K., Kim, M., Chen, Y.R., 2002. Detection of defects on selected apple cultivars using hyperspectral and multispectral image analysis. Applied Engineering in Agriculture 18 (2), 219–226.

Mehl, P.M., Chen, Y.R., Kim, M.S., Chan, D.E., 2004. Development of hyperspectral imaging technique for the detection of apple surface defects and contaminations. Journal of Food Engineering 61 (1), 67–81.

Nagata, M., Tallada, J.G., Kobayashi, T., Toyoda, H., 2005. NIR hyperspectral imaging for measurement of internal quality in strawberries. ASAE Paper No. 053131, ASAE Meeting, Tampa, FL, USA.

Park, B., Chen, Y.R., 1996. Multispectral image analysis using neural network algorithm. ASAE Paper No. 96-3034.

Park, B., Windham, W.R., Lawrence, K.C., Smith, D.P., 2004. Hyperspectral image classification for fecal and ingesta identification by spectral angle mapper. ASAE Paper No. 043032, ASAE/CSAE Meeting, Ottawa, Ont., Canada.

Polder, G., van der Heijden, G.W.A.M., Young, I.T., 2002. Spectral image analysis for measuring ripeness of tomatoes. Transactions of the ASAE 45 (4), 1155–1161.

Skog, L.J., 1998. Chilling Injury of Horticultural Crops. Food and Rural Affairs, Report No. 98-021, Ontario Ministry of Agriculture, Canada.

Vízhányó, T., Felföldi, J., 2000. Enhancing colour differences in images of diseased mushrooms. Computers and Electronics in Agriculture 26 (2), 187–198.

Watkins, C., Jackie Nock, J., 2004. SmartFreshTM (1-MCP)—the good and bad as we head into the 2004 season. New York Fruit Quarterly 12 (3), 1–26.

Xing, J., De Baerdemaeker, J., 2005. Bruise detection on 'Jonagold' apples using hyperspectral imaging. Postharvest Biology and Technology 37 (1), 152–162.